Journal of Information Systems Engineering and Management
2025, 10(35s)
e-ISSN: 2468-4376
https://www.jisem-journal.com/

Research Article

Effect of Perforated Pin Fin on Thermal Performance of a Rectangular Channel in Forced Convection

Anssam Ali [1], Ali Sabri [2*]
[1] *Mechanical engineering, nahrain University, baghdad-iraq . Anssamalio@gmail.com*
[2] *Mechanical engineering, nahrain University, baghdad-iraq . ali.s.abbas@nahrainuniv.edu.iq.*

ARTICLE INFO

Received: 22 Dec 2024

Revised: 14 Feb 2025

Accepted: 26 Feb 2025

ABSTRACT

The focus of this study is to characterize the thermal behaviour of a planar heat sink with different fin patterns, namely solid, perforated, and taper fins in both inline and staggered orientations under horizontal fluid flow conditions. By using computational fluid dynamics (CFD) simulations within ANSYS software to validate the numerical model with experimental one, the study explores how adjustments to fin designs can improve heat transfer efficiency. It confirms that changes in fin profile have substantial effects on thermal performance by effectively enlarging the area for heat exchange as well as promoting turbulence. Although the study shows that increasing heat transfer area is essential, puncturing the fin structure accelerates fluid flow and enhances thermal efficiency. Overall, twelve different fin configurations, solid and perforated square fins together with diamond-shaped ones (solid & incrementally pierced on the base), edge-perforated in addition to a hollow internal rectangular cross-section of a passage, were investigated. The main objective is evaluating key performance parameters such as Nusselt number, friction factor, and heat transfer effectiveness. The results demonstrate that the higher heat transfer effectiveness factor is about 1.55 for perforated diamond fins and 1.5 for perforated fins, while the lowest value is 0.8 for solid diamond fins.

Keywords: Heat sink, thermal performance, perforated fins, turbulence, CFD.

INTRODUCTION

As electronic devices have expanded and the search for the best ways to cool them has escalated over the last decade, researchers have focused on the heat sink and how to improve it. Following are the previous experimental and computational investigations conducted on heat sinks.

Choudhary et al. [1] studied experimentally the airflow characteristics of pin fin heat sinks (PFHS) with and without wings under forced convection. For both inline and staggered pin fin designs, the fin pitch ratio (S/D) and wing size ratio (Lw/D) were adjusted for the Re range of 6800-15,100. They discovered that the most efficient performance is achieved by a PFHS with wings, with an Lw/D ratio of 0.2 and a S/D ratio of 2. Hatem et al. [2] conducted an experimental study investigating heat exchange in a circular perforated pin fin heat sink (PPFHS). They observed that non-perforated fins experienced a temperature reduction from 35°C to 31°C at a power level of 10 W, whereas perforated fins experienced a temperature drop from 35°C to 29.8°C. Also, through an experimental investigation, Jassem [3] assessed the heat transfer through natural convection in rectangular perforated fin plates. He used five fins, one non-perforated and four perforated by circle, square, triangular, and hexagon forms, all with the same cross-section area (113 mm^2). The investigation revealed that the heat transfer coefficient of triangular perforation is the highest, followed by circular, square, hexagonal, and non-perforation. Mohammed et al. [4] conducted a study investigating how modifying the shape and pattern of rectangular fins affects heat transfer efficiency and effectiveness. The goal was to identify the most effective perforation shape for enhancing heat transfer. The findings indicated that the temperature distribution of fins with perforations had a more pronounced temperature reduction than fins without perforations, with triangular hole perforation exhibiting a 78.98% higher heat transfer coefficient.

Bakhti et al. [5] performed a computational investigation on the turbulent flow of nanofluids in heat sinks with perforated circular fins. The study utilized TiO_2, Al_2O_3, and Cu nanofluids as cooling fluids. The selected nanofluids had volumetric concentrations ranging from 2% to 10%. The findings demonstrated a notable

Journal of Information Systems Engineering and Management
2025, 10(35s)
e-ISSN: 2468-4376
https://www.jisem-journal.com/

Research Article

enhancement in thermal transfer in comparison to the use of water alone. Additionally, research has been conducted on improving heat transfer in solar air heaters using baffles Abbas et al. [6] Maji et al. [7] developed a 3D CFD model of heat sinks for pierced pin fins of different forms, specifically emphasizing the fin shape, puncture geometry, and puncture size. The researchers discovered that perforated fins dissipate heat faster than non-perforated fins, and this heat dissipation rate increased dramatically as the shape of the holes and fins were altered. Maleki et al. [8] numerically examined the impact of perforation shape on the characteristics of smooth and continuous airflow and heat transfer properties across a PPFHS. They established a 3D simulation model using the finite-volume method and the SIMPLE algorithm. Using circular perforations resulted in the highest efficiency when considering the heat transfer surface area for perforated fins. Sahel et al. [9] performed a numerical study to determine the optimal arrangement of hemispherical pin fins (HSPFs) and their hydrothermal performance on a heat sink in a fully turbulent flow. The numerical approach of the proposed heat sink was tested using a heat sink with staggered cylindrical pin fins. The researchers discovered that the highest heat transfer performance factor (HTPF) achieved was 1.87. This was obtained with a ratio of the diameter to the hydraulic diameter of 0.833 and a Re of 21,367. In comparison to the reference case, the heat sink volume was reduced by 76% by the HSPF design.

Multiple studies examined the performance of perforated fins heat sinks in experimental and computational analyses [10]–[14]. Song et al. [15] analyzed the heat dissipation of a heat sink with perforated fins on a cylindrical base through a numerical analytical approach validated experimentally. They discovered that increasing the number of small holes improved the heat dissipation. Ibrahim et al. [16] conducted a comparative analysis of the effectiveness of fins in enhancing forced convection heat transfer, both with and without perforated geometries. The findings from the experiments and the calculations coincided exceptionally well. Perforated fins exhibited superior thermal performance to non-perforated fins, resulting in an 8.5°C reduction in fin temperature. They exhibited excellent results in hydraulic performance, particularly with increasing perforations. Hussein et al. [17] examined the impact of recently suggested tile fin designs on the thermal conductivity of a heat sink under natural convection conditions. The results were validated using a theoretical correlation showing satisfactory agreement with an acceptable percentage error deviation. The heat sink with fins achieved thermal equilibrium more rapidly and at a lower temperature than without fins. Shaeri et al. [18] performed a validated numerical study on fluid flow and concomitant conduction-convective heat transfer. They used a three-dimensional array of rectangular perforated fins with square windows positioned numerically on the lateral surface of the fins. It was discovered that recently improved fins exhibit more total heat transfer and are significantly lighter compared to solid fins. Shaeri et al. [19] undertook a meticulous investigation to investigate the three-dimensional, non-compressible, smooth fluid flow and heat transmission of a heated arrangement of rectangular fins, both with holes and without, attached to a flat surface. Perforated fins exhibit exceptional performance, and their effectiveness is further boosted by augmenting the quantity of perforations. Bin Samsudin et al. [20] conducted an analysis of the heat transfer and fluid flow in various novel heat sink configurations. Integrating wings onto pin fins greatly enhanced heat dispersion from regions experiencing elevated temperatures. Implementing the Perforated Hollow Pin-Fin Heat Sink (PHPFHS) led to a significant 47% improvement in heat transfer compared to the configuration lacking wings.

Based on the literature, introducing perforations in the fin structure induces turbulence, thereby enhancing thermal efficiency levels and potentially reducing the overall cost of the heat sink. Consequently, this study examines the thermal performance of a planar heat sink featuring various fin configurations, including solid, perforated, and tapered fins, arranged in two typical orientations (inline and staggered) under horizontal fluid flow conditions. The investigation seeks to quantify the impact of these design variations on heat dissipation efficacy and overall thermal management, employing computational fluid dynamics (CFD) simulations to model the heat transfer and fluid flow characteristics of each design variant. By analyzing key parameters such as fin geometry, perforation patterns, and orientation, this research attempts to elucidate the most effective configuration for specific application scenarios, ultimately contributing to developing more efficient and cost-effective thermal management solutions for electronic devices and industrial applications Previous studies have also explored heat diffusion in various materials, including prosthetics Abbas and Dawood. [21] . The study proposes 12 diverse new pin fin models that incorporate the effects of fin shape, orientation, and modification. The novel proposed and analyzed fin designs in this study aim to enhance the heat transfer performance of heat sinks, providing valuable insights for designing efficient thermal management solutions.

2. MODEL DESCRIPTION

In Ansys, the geometry was generated using Space Claim. The computational domain was transferred to the meshing program in Ansys workbench, with a density of three times doubling the mesh's density for similar results. The mesh had 2,500,000 elements covering the heat sink and surrounding flow domain, as shown in

Journal of Information Systems Engineering and Management
2025, 10(35s)
e-ISSN: 2468-4376
https://www.jisem-journal.com/

Research Article

Fig.1. The mesh was imported into Ansys Fluent 2023 R2, which was used for steady-state simulation with pressure-based algorithms, considering gravity, continuity, momentum, and energy equations. Air and aluminium were used, and boundary conditions were imposed for each face. The simulations started with small residuals, and the flow experienced swirls, separations, reattachments, and impingements.

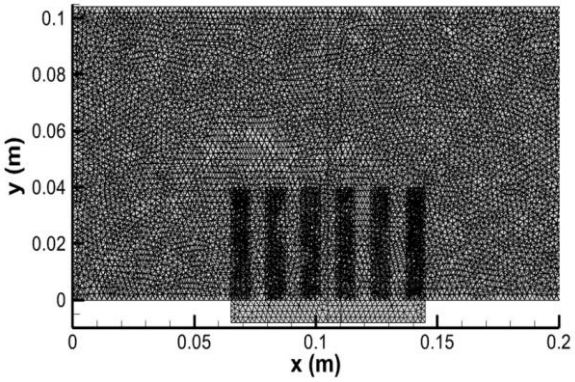

Figure (1): Computational mesh generated for the cases of numerical validation.

2.2 Proposed Geometries

The goal of all studies is to incorporate the effect of the far-field stream cooling down the solid to such a degree that is desirable for the material from the design point of view. The current study is devoted to establishing new pin fins models for that purpose. It deals with the fin's shape, orientation, and modification rather than the flow passage. The primary geometry used for this study is square with a 50 (mm) length. It is assumed there are 64 fins distributed equally over the plate, and the flow is directed along the axial side only. Since the flow is symmetrical with a Z-axis, one row of 8 fins will be simulated**.** Similar approaches have been applied to enhance the performance of plate-fin heat exchangers using vortex generators Abbas and Mohammed.[22]. Fig.2 shows all simulations' dimensions, including 12 different cases.

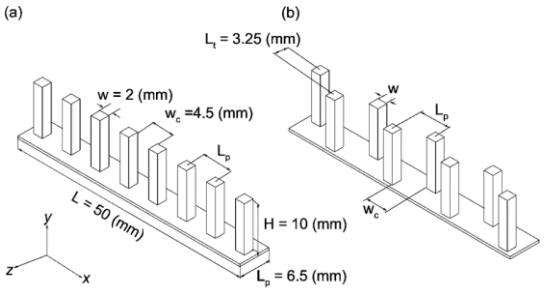

Figure (2): The basic shape, orientation, number, and dimensions of the fin utilized for the current study with two arrangements: (a) inline and (b) staggered.

Fig.3 illustrates the proposed modifications to the pin fin construction. This type of geometric manipulation can be found in existing literature; however, it may include different design recommendations or be intended for alternative uses.

Journal of Information Systems Engineering and Management
2025, 10(35s)
e-ISSN: 2468-4376
https://www.jisem-journal.com/

Research Article

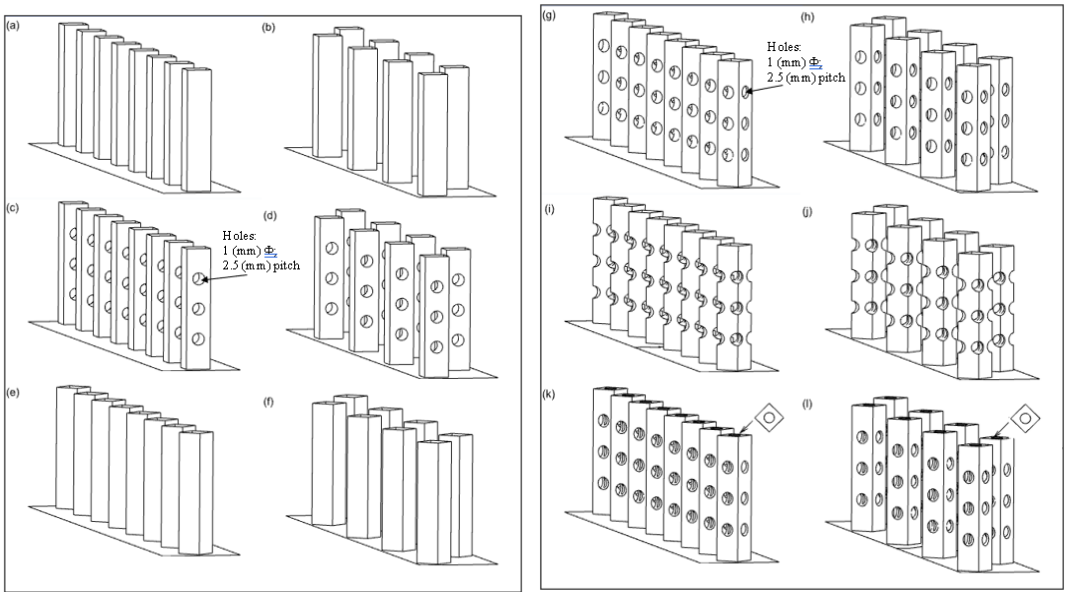

Figure (3): The new models proposed for the current study as test cases for thermal performance improvements (solid square fin (a,b), perforated square fin (c,d), solid diamond fin (e,f), perforated diamond fin (g,h), edge-perforated diamond fin (i,j), and hollow, perforated diamond fin (k,l).

To simulate the air around the fins, a domain of 3 L and ($\boldsymbol{w_c + w}$) was assigned for all cases above. Fig.4 shows this domain with air surrounding the solid of the current study. The homogenous heat flux is directed from the bottom to all the heat sink surfaces with L length. This length was extended once more in the upstream and doubled in the downstream. The flow is axial and enters as a fully developed flow with uniform velocity.

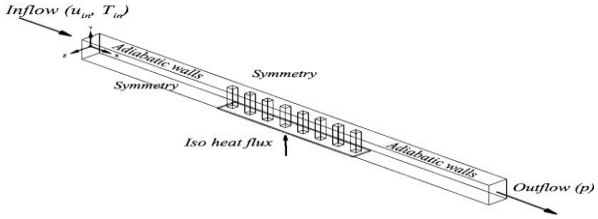

Figure (4): Computational domains for the solid and surrounding air; this is for illustration, not accurate dimensions.

2.2.1 Mesh quality and adequacy

The study analyzed meshes with varying elements to achieve mesh independence. The boundary conditions were set with the highest Reynolds number, 6580. The meshing process included both air and solid domains. Fig.5 shows a curve for the thermal resistance (R_th) with respect to the number of elements. The thermal resistance (R_th) was measured with 141535 elements, then doubled to 512020. Some tests showed sharp changes in R_th values, requiring further testing to reach good quality.

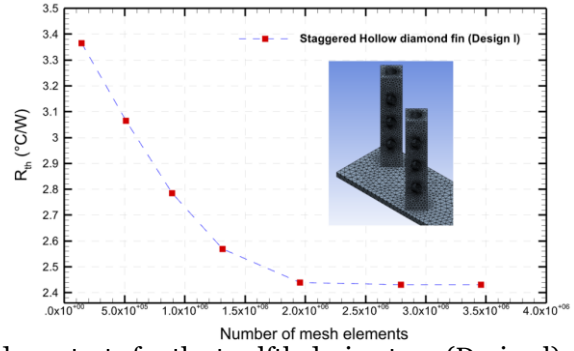

Figure (5): Mesh independence tests for the twelfth design type (Design l) regarding thermal resistance.

2.3 Numerical Validation

The geometric properties and other parameters are depicted in Fig.1.

Journal of Information Systems Engineering and Management
2025, 10(35s)
e-ISSN: 2468-4376
https://www.jisem-journal.com/

Research Article

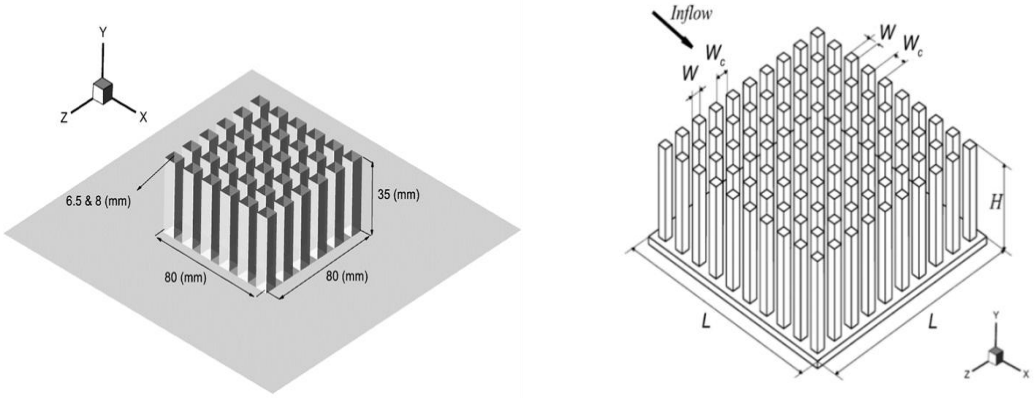

Figure (6): Main dimensions of the experimental geometry [20] for validation.

Two experimental instances, a 6.5 mm square fin and an 8 mm square fin, were chosen from [20] to validate the numerical solution. The experiment was designed using a square base plate and square fins. The heat sink of [20] comprised a jet that directed airflow through the fin banks, a square metal base, and fins. Fig.6 displayed a total of 36 pin fins arranged around the base. The base has a length of 80 mm (L), a height of 35 mm (H), a fin width of either 6.5 mm or 8 mm (w), and a base height of 8 mm (b). For this validation, all the distances were measured in a manner similar to those in [23]. In the experiment conducted in [23], the flow was disrupted at various speeds in all directions of the plate.
The experiment's data were taken at two fin widths (6.5 and 8 mm). Then, the simulations were conducted for these two cases with the same boundary conditions. It attempts to mimic the experiment precisely so that the results are identical. The comparison was performed regarding thermal resistance, R_{th}, and Reynolds number, Re. As presented in [23] 's experiment, five tests were conducted for five Re, plotted in Fig.7 with symbolled and dashed lines. The current numerical values are plotted with solid lines in the same figure for comparison.

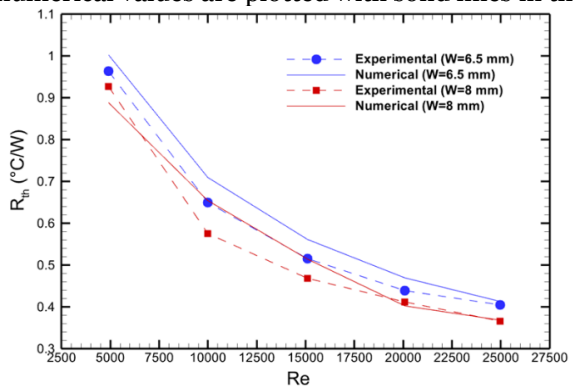

Figure (7): Numerical results validated against the experiment [20] for two cases of fin width.

3. DATA REDUCTION

The Reynolds-averaged Navier-Stokes equations will be applied to modelling turbulence. Several studies showed that reliable results can be achieved when using the k-ε turbulent model for this kind of flow. Thus, the momentum energy equations of this model are the set of formulas that regulate the fluid herein, and they are [24].
Momentum equation for the fluid,

$$\frac{\partial}{\partial x_j}\left(\rho u_i u_j\right) = -\frac{\partial p}{\partial x_i} + \frac{\partial}{\partial x_j}\left[(\mu + \mu_t)\left(\frac{\partial u_i}{\partial x_j} + \frac{\partial u_j}{\partial x_i}\right) - \frac{2}{3}\mu\delta_{ij}\frac{\partial u_l}{\partial x_l}\right] \quad (1)$$

The energy equation for the fluid,

$$\frac{\partial}{\partial x_i}\left[u_i(\rho E + p)\right] = \frac{\partial}{\partial x_i}\left[\left(k_f + k_t\right)\frac{\partial T}{\partial x_i}\right] + S_b \quad (2)$$

The symbol ρ represents the density, while u_i is the velocity component. Other parameters such as p, μ, and μ_t are the static pressure, molecular viscosity, and turbulent viscosity. For the energy field, E represents the total

Journal of Information Systems Engineering and Management
2025, 10(35s)
e-ISSN: 2468-4376
https://www.jisem-journal.com/

Research Article

energy, k_f the thermal conductivity of the fluid, k_t the turbulent conductivity, S_b The energy generation rate per unit volume, and T the temperature.

The general form of the heat conduction equation for the solid side is

$$\frac{\partial}{\partial x_i}\left(k_s \frac{\partial T}{\partial x_i}\right) + S_b = 0 \quad (3)$$

where k_s is the thermal conductivity of the solid. Therefore, the two heat transfer mechanisms that contribute to the cooling of heat plates are conduction and convection. From the energy balance, it can be derived the convection heat transfer formula as follows:

$$Q = hA_t(T_{\text{ave}} - T_\infty) \quad (4)$$

where T_{ave} is the average temperature of the heat sink and T_∞ is the temperature of the free stream. The symbol A_t denotes the total heat transfer area, which includes the upper face of the plate base and total fin areas, i.e., $A = L^2 + 4nwH$. Here, L is the length of the base plate ($L = \mathrm{L} - n_{\text{row}}\,\mathrm{w}$), n is the fin number while n_{row} is for one row, w is the fin width, and H is the fin height. The following equation is written as a user-defined function for ANSYS to illustrate results.

Heat transfer coefficient
$$h = \frac{Q}{A_t(T_{\text{ave}} - T_\infty)} \quad (5)$$

Thermal resistance
$$R_{th} = \frac{T_{ave} - T_\infty}{Q} = \frac{1}{hA_t} \quad (6)$$

Reynolds number
$$\mathrm{Re} = \frac{u_{in}\, D_h}{\nu_f} \quad (7)$$

Friction factor
$$f \equiv \frac{\Delta p}{0.5\rho u_{in}^2} \cdot \frac{D_h}{4L} \quad (8)$$

Nusselt number
$$\mathrm{Nu} = \frac{hD_h}{k_f} \quad (9)$$

Effectiveness factor (η_{eff})
$$\eta_{\text{eff}} = \frac{\mathrm{Nu}/\mathrm{Nu}_\infty}{(f/f_\infty)^{1/3}} \quad (10)$$

4. RESULTS AND DISCUSSION

The purpose of this study is to present and analyze the outcomes of the twelve novel designs and arrangements. These outcomes will be expressed in terms of key parameters, including fin efficiency, thermal resistance, Nusselt number, and friction factor, among others.

4.1 Temperature and pressure contours

Fig.8 displays temperature distributions across the twelve different heat sink scenarios. As observed, the figure uncovers notable variations in temperature within the heat sink under low incoming air temperature conditions. The temperature difference between the air and the heat sink's average temperature directly influences the heat sink's thermal efficiency. Using square fins arranged in a queuing inline configuration results in a temperature increase of 80°C above the average sink temperature. On the other hand, the use of staggered fins reduces the temperature to below 80°C. The diamond fin performs superior to square fins in the inline configuration, achieving temperatures ranging from 80°C to 65°C or lower. The temperature distribution of perforated diamond fins exhibits a temperature range of 35 to 65°C for the inline configuration and 35 to 50°C for the staggered layout. For designs (g-l), such as grid-like, edge, and hollow fins, heat sinks typically have temperature ranges of 35 to 65 °C for inline arrangements and 35 to 50 °C for staggered configurations. This exemplifies the efficacy of integrating perforations in fins, as they diminish the temperature of the heat sink, hence enhancing thermal efficiency.

Journal of Information Systems Engineering and Management
2025, 10(35s)
e-ISSN: 2468-4376
https://www.jisem-journal.com/

Research Article

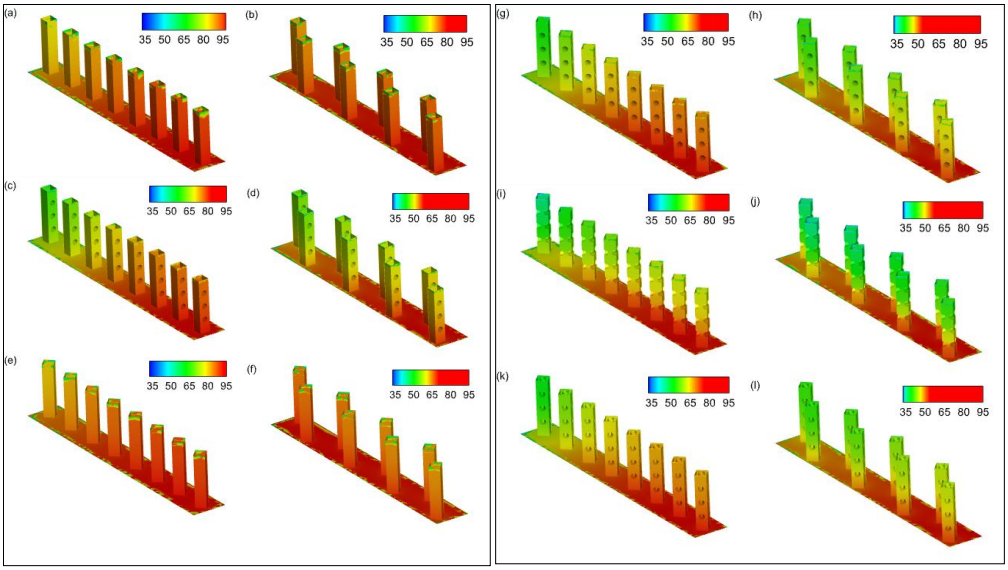

Figure (8): Temperature contours for the two arrangements: solid square fin (a,b), perforated square fin (c,d), solid diamond fin (e,f), perforated diamond fin (g,h), edge-perforated diamond fin (i.j), and hollow, perforated diamond fin (k,l).

The fin distributions considerably impact the flow losses in a heat sink. Fig.9 displays pressure distributions across the twelve different heat sink scenarios. The initial three suggested designs, namely the solid square fin (a,b), perforated square fin (c,d), and solid diamond fin (e,f), demonstrate that staggered patterns yield higher losses compared to inline patterns. The presence of perforations in the fin design decreases pressure drop, whereas the inclusion of diamond shapes results in increased pressure losses. The staggered arrangement of solid diamond fins does not encounter negative pressure. The remaining fin designs, namely the perforated diamond fin (g,h), edge-perforated diamond fin (i,j), and hollow, perforated diamond fin (k,l), demonstrate that the flow becomes increasingly disrupted and undergoes a reduction in speed as it encounters the walls of the diamond fins. Perforations improve the flow, whereas staggeration does not produce the same outcome. The presence of holes at the edges of the design results in more significant pressure drops. However, this scenario may be preferable when taking into account the pressure drop.

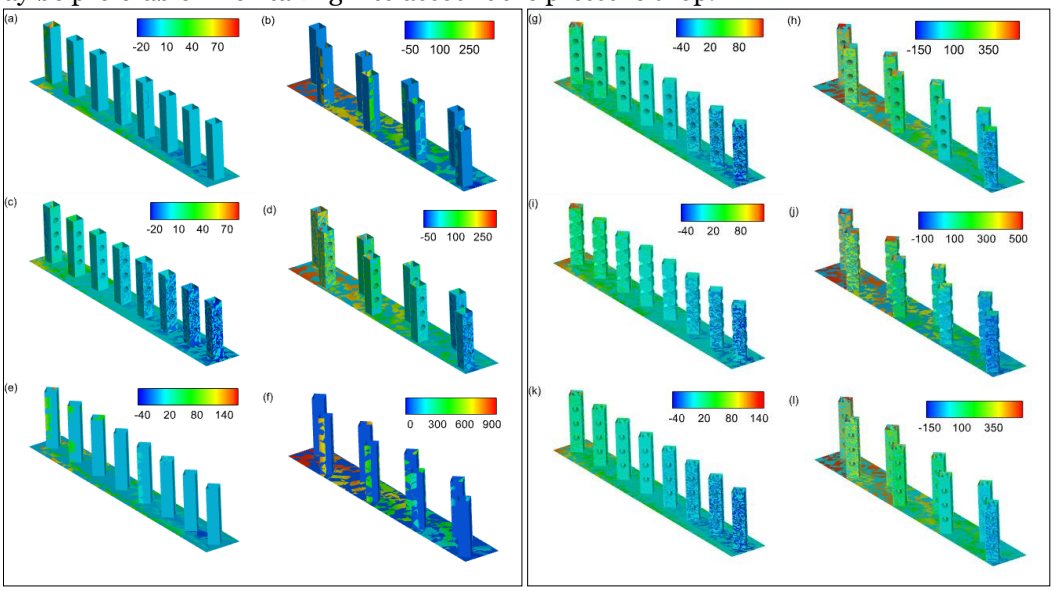

Figure (9): Total pressure contours for the two arrangements: solid square fin (a,b), perforated square fin (c,d), solid diamond fin (e,f), perforated diamond fin (g,h), edge-perforated diamond fin (i.j), and hollow, perforated diamond fin (k,l).

Journal of Information Systems Engineering and Management
2025, 10(35s)
e-ISSN: 2468-4376
https://www.jisem-journal.com/

Research Article

4.2 Average heat transfer coefficient

In order to consider the magnitude of convection heat transfer, mean values of heat transfer coefficients were generated for all of the test cases. Fig.10, which is presented in the form of a graphical representation, provides a visual depiction of the variations in average heat transfer coefficients as they relate to the Reynolds number. It is worth noting that this figure has been divided into two distinct categories for the sake of clarity and organization. Specifically, Fig.10a represents the inline arrangement, while Fig.10b pertains to the staggered pattern. Upon examination of the figure, it becomes evident that the heat transfer coefficient experiences an upward trend as the Reynolds number increases. This phenomenon can be attributed to the presence of heightened flow momentum, which in turn influences the viscous effects. Additionally, a noteworthy observation can be made regarding the disparity in thermal convection between flows surrounding the inline fins and those surrounding the staggered fins. The impact of passive enhancements has also been studied in solar applications Jebir et al.[25].

When focusing on Fig.10a, it becomes apparent that the curves depicted within the graph provide further confirmation of the superiority of diamond designs in terms of heat transfer rate when compared to square designs. Furthermore, it is worth mentioning that the performance of solid unperforated fins falls short in comparison to perforated fins. Notably, the perforated diamond fin boasts the highest values of heat transfer coefficients, reaching approximately 250 (W/m². ºC). It is closely followed by the edge-perforated diamond fin. On the other hand, the heat transfer achieved by a perforated square fin exceeds that of a hollow, perforated diamond fin. This distinction can be attributed to the fact that vertical holes within the structure of the fin have the potential to hinder the heat transfer mechanism by reducing the area available for heat transfer.

Fig.10b exhibits the opposite aspect of augmenting heat transfer by amplifying the area of circulations, which includes more obstacles. This particular figure once again showcases the perforated diamond fin (design f) as the superior choice, as it possesses a heat transfer coefficient of approximately 375 (W/m2. ºC). This signifies a considerable 50% augmentation in comparison to a linear arrangement.

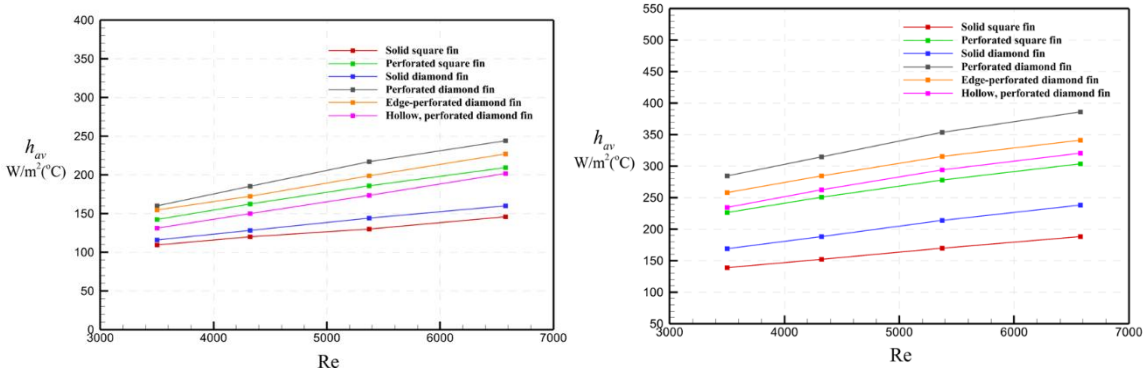

Figure (10): (a) Heat transfer coefficient versus Reynolds number for inline fin arrangement and (b) Heat transfer coefficient versus Reynolds number for staggered fin arrangement.

4.3 Average Nusselt number

Illustrated in Fig.11 are the values of the Nusselt number in relation to the Reynolds numbers, which are graphically depicted for the six cases with an inline arrangement in Fig.11a. The curves exhibit a predictable ascent in conjunction with the increase in the Reynolds number. Figure 10b, on the other hand, presents the Nusselt numbers for the sixth staggered fins, as denoted in the accompanying legends. Through an analysis of the heat transfer values, it has been determined that the most effective design for heat transfer is the perforated diamond fin, surpassing all other design options.

Based on this finding, we can draw the conclusion that the staggered, perforated diamond fin provides the greatest enhancement in Nusselt, with an approximate 70% increase compared to the inline, perforated diamond fin. Additionally, it is noteworthy that the hollow, staggered, perforated fins outperform their inline counterparts, while both types demonstrate superior performance compared to the solid square and diamond fins. In conclusion, according to the definition, the Nusselt number rises when flow velocity surpasses the viscous effect. Because of this, as the hole raises the flow velocity, the perforated fins function better. As with the diamond fins, creating a sharp edge in front of the approaching flow also enhances velocity.

Journal of Information Systems Engineering and Management
2025, 10(35s)
e-ISSN: 2468-4376
https://www.jisem-journal.com/

Research Article

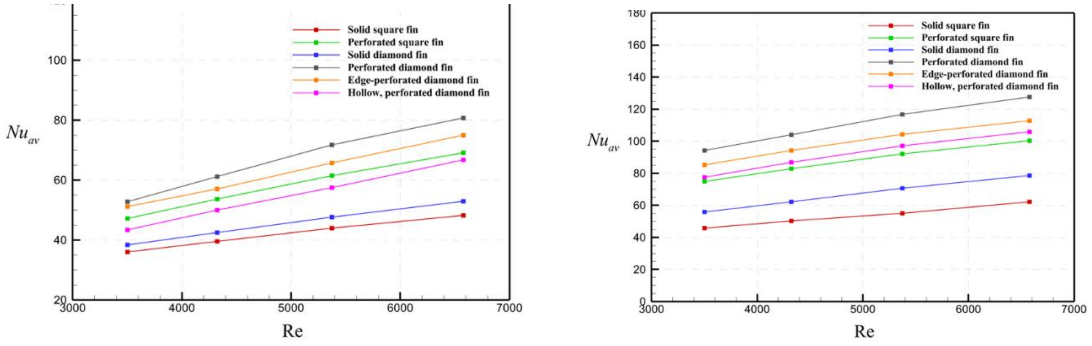

(a) **(b)**

Figure (11): (a) Nusselt numbers with Reynolds number for inline fin arrangement and (b) Nusselt numbers with Reynolds number for staggered fin arrangement.

4.4 Friction factor

Increasing the airflow over the heat sink leads to increased flow losses, particularly in situations where there are numerous obstructions present. This subsequently necessitates a greater amount of energy to facilitate the flow and extract additional energy. From a design perspective, it is imperative to take into account both the thermal Nusselt number, denoted as (Nu), and the hydraulic friction factor, represented by (f_c). For illustrative purposes, Fig.12 provides a compilation of calculated data pertaining to the aforementioned variables for the inline flow across a diverse range of six distinct fin types.

Notably, it is worth mentioning that the perforated fins in this particular context exhibit a distinct style that diverges from the previously observed results. It is important to highlight that the square fin, as opposed to the diamond fin, demonstrates superior performance in terms of minimizing friction losses. This can be attributed to its ability to maintain a more uniform flow, thus promoting a more efficient transfer of fluid. Additionally, it is worth noting that the presence of perforations in the diamond fin leads to slightly higher losses compared to fins with perforations located at either the edges or the interior of the fin. Consequently, the optimal performance is achieved by the perforated square fin. Not only does it ensure a uniform flow, but the perforations also contribute to enhancing the overall flow and reducing losses. Lastly, it is pertinent to acknowledge the significant disparity observed in the figure between all square fins and diamond fins.

Fig.12b visually displays the numerical values pertaining to the various fin designs. In a general sense, the values have been augmented twofold due to the occurrence of zigzag flow, which leads to an increased flow loss. Additionally, in the case of Fig.12b, there are nearly identical disparities observed between the different types of fin shapes, similar to those observed in Fig.12a. Nevertheless, it is imperative to note that the trends depicted in both figures remain consistent and exhibit minimal variation with changes in Reynolds number. It is widely recognized that at higher air velocities, the frictional forces should decrease as a result of the reduced viscous effect. However, this phenomenon does not hold true for the heat sink being examined in this instance. Consequently, the friction factor increases since the fraction factor is the product of the shear stress and the flow velocity. Due to strong shear forces between the flow and the solid walls, this is evident in the situations of perforation, diamond shape, and staggered alignment, where the friction factor rises more than it does in other situations.

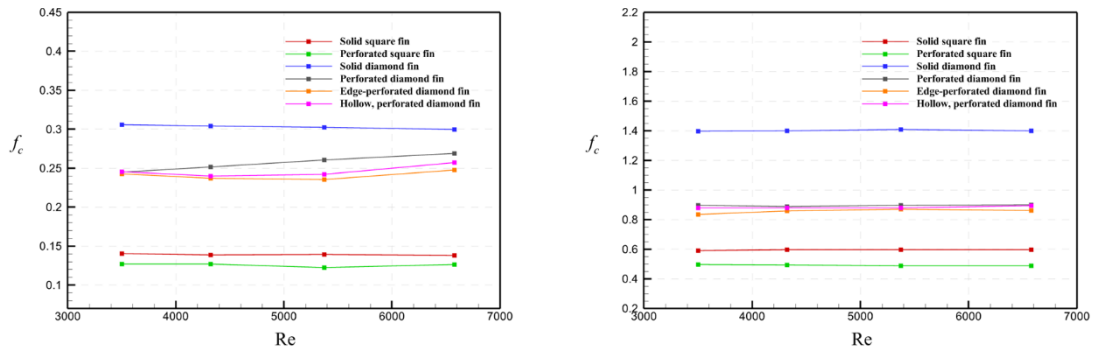

(a) **(b)**

Figure (12): (a) Friction factor versus Reynolds number for inline fin arrangement and (b) Friction factor versus Reynolds number for staggered fin arrangement.

Journal of Information Systems Engineering and Management
2025, 10(35s)
e-ISSN: 2468-4376
https://www.jisem-journal.com/

Research Article

4.5 Heat transfer effectiveness factor

Fig.13 illustrates the thermal performance over the Reynolds number. Interestingly, the edge-perforated diamond fin demonstrates a superior performance when compared to the internally perforated version, as demonstrated in the accompanying figure. Lastly, it is essential to note that the values range from 1.3 to 1.5 within this specific context. On the other hand, it is manifestly clear, as depicted in Fig.13b, that when it comes to performance, solid fins exhibit superior results when they are arranged in a linear fashion rather than staggered. This is evidenced by the fact that the values in Fig.13b show a decrease of approximately 20% for these types of solid fins, as indicated by the red and blue curves. In stark contrast, the perforation factor plays a significant role in enhancing heat transfer and improving the overall effectiveness. This can be observed by examining the green, black, orange, and pink curves. Among these, the perforated diamond fin demonstrates the highest level of effectiveness. Furthermore, considering staggered alignments, it is noteworthy that there is a substantial percentage increase of approximately 10% in the values of the heat transfer effectiveness factor.

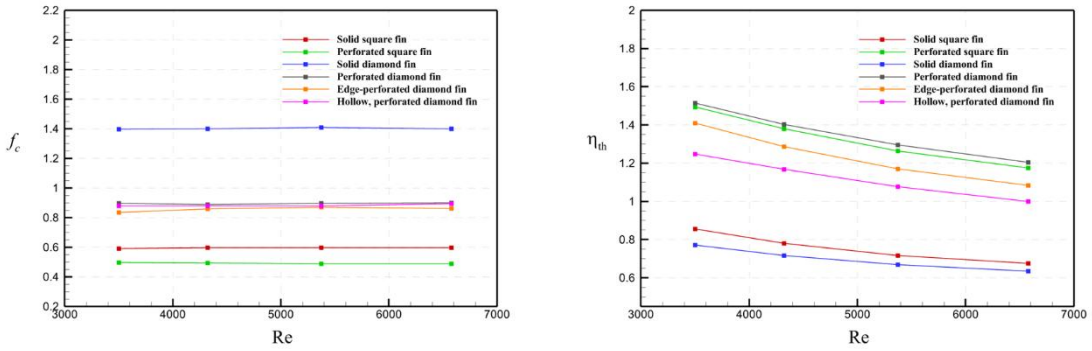

(a) **(b)**

Figure (13): (a) Heat transfer effectiveness factor versus Reynolds number for inline fin arrangement and (b) Heat transfer effectiveness factor versus Reynolds number for staggered fin arrangement.

5. CONCLUSION

This study aimed to investigate the thermal performance of a planar heat sink with various fin configurations under horizontal fluid flow conditions. Twelve distinct fin designs were examined, including solid, perforated, and tapered fins in both inline and staggered orientations. The research objectives were to evaluate the impact of fin geometry, perforation patterns, and orientation on heat dissipation efficacy and overall thermal management.

KEY FINDINGS FROM THIS INVESTIGATION INCLUDE:

- Fin modification significantly enhances thermal behaviour. Altering fin orientation and structure while maintaining extended areas resulted in notable increases in effectiveness.
- Perforations in the fin structure induce turbulence, thereby boosting thermal efficiency. This strategy elevates heat sink efficiency and potentially reduces overall production costs.
- Among the twelve geometries examined, the perforated diamond fin in a staggered arrangement (design h) demonstrated superior performance. This configuration achieved the highest heat transfer coefficient, approximately 375 W/m²·°C, representing a 50% improvement over its inline counterpart.
- The staggered, perforated diamond fin also exhibited the greatest enhancement in Nusselt number, with an approximate 70% increase compared to the inline, perforated diamond fin.
- In terms of the heat transfer effectiveness factor, the perforated diamond fin in a staggered arrangement consistently outperformed other designs across various Reynolds numbers.
- While perforated designs generally showed improved thermal performance, they also exhibited slightly higher friction factors, particularly in staggered arrangements.
- This study did not investigate entirely new configurations of pin fins but rather focused on comparing and optimizing existing designs. The findings provide valuable insights for designing more efficient and cost-effective thermal management solutions for electronic devices and industrial applications. Future research could explore novel fin geometries or hybrid designs that further optimize the balance between heat transfer enhancement and pressure drop.

REFERENCES:

[1] V. Choudhary, M. Kumar, and A. K. Patil, "Experimental investigation of enhanced performance of pin fin heat sink with wings," *Appl. Therm. Eng.*, vol. 155, pp. 546–562, 2019.
[2] M. Hatem, H. Abdellatif, and W. Hussein, "Enhancement of perforated pin-fins heat sink under forced convection," *Int. Res. J. Eng. Technol.*, vol. 7, no. 10, pp. 1440–1445, 2020.
[3] R. R. Jassem, "Effect the form of perforation on the heat transfer in the perforated fins," *Acad. Res. Int.*, vol. 4, no. 3, p. 198, 2013.
[4] M. Mohammad, M. P. H. Talukder, K. A. Rahman, and M. W. Hridoy, "Experimental investigation on the effect of different perforation geometry of vertical fins under forced convection heat transfer," in *International Conference on Mechanical Engineering and Renewable Energy*, 2019, pp. 11–13.
[5] F. Z. Bakhti and M. Si-Ameur, "A comparison of mixed convective heat transfer performance of nanofluids cooled heat sink with circular perforated pin fin," *Appl. Therm. Eng.*, vol. 159, p. 113819, 2019.
[6] Abbas, A.S., Mahmoud, M.S., Khudheyer, A.F. (Year). Improvement of heat transfer for airflow through a solar air heater channel with cutoff desecrate baffles. Journal Name, Volume(Issue), Page range.
[7] A. Maji, D. Bhanja, and P. K. Patowari, "Numerical investigation on heat transfer enhancement of heat sink using perforated pin fins with inline and staggered arrangement," *Appl. Therm. Eng.*, vol. 125, pp. 596–616, 2017.
[8] H. Maleki, M. R. Safaei, A. S. Leon, T. Muhammad, and T. K. Nguyen, "Improving shipboard electronics cooling system by optimizing the heat sinks configuration," *J. Ocean Eng. Sci.*, vol. 7, no. 5, pp. 498–508, 2022.
[9] D. Sahel, L. Bellahcene, A. Yousfi, and A. Subasi, "Numerical investigation and optimization of a heat sink having hemispherical pin fins," *Int. Commun. Heat Mass Transf.*, vol. 122, p. 105133, 2021.
[10] A. J. Obaid and V. M. Hameed, "An experimental and numerical comparison study on a heat sink thermal performance with new fin configuration under mixed convective conditions," *South African J. Chem. Eng.*, vol. 44, no. 1, pp. 81–88, 2023.
[11] N. A. Ghyadh, S. S. Ahmed, and M. Al-Baghdadi, "Enhancement of forced convection heat transfer from cylindrical perforated fins heat sink-CFD study," *J. Mech. Eng. Res. Dev.*, vol. 44, no. 3, pp. 407–419, 2021.
[12] N. R. Noori and A. F. Saeed, "The Experimental Impact of Convective Heat Transfer Improvement from Numerous Perforated Shape Fin Array," *Al-Rafidain Eng. J.*, vol. 28, no. 1, pp. 280–292, 2023.
[13] T. K. Ibrahim, A. T. Al-Sammarraie, M. S. M. Al-Jethelah, W. H. Al-Doori, M. R. Salimpour, and H. Tao, "The impact of square shape perforations on the enhanced heat transfer from fins: Experimental and numerical study," *Int. J. Therm. Sci.*, vol. 149, p. 106144, 2020.
[14] S.-B. Chin, J.-J. Foo, Y.-L. Lai, and T. K.-K. Yong, "Forced convective heat transfer enhancement with perforated pin fins," *Heat Mass Transf.*, vol. 49, pp. 1447–1458, 2013.
[15] G. Song, D.-H. Kim, D.-H. Song, J.-B. Sung, and S.-J. Yook, "Heat-dissipation performance of cylindrical heat sink with perforated fins," *Int. J. Therm. Sci.*, vol. 170, p. 107132, 2021.
[16] T. K. Ibrahim *et al.*, "Experimental and numerical investigation of heat transfer augmentation in heat sinks using perforation technique," *Appl. Therm. Eng.*, vol. 160, p. 113974, 2019.
[17] M. A. Hussein, V. M. Hameed, and H. T. Dhaiban, "An implementation study on a heat sink with different fin configurations under natural convective conditions," *Case Stud. Therm. Eng.*, vol. 30, p. 101774, 2022.
[18] M. R. Shaeri, M. Yaghoubi, and K. Jafarpur, "Heat transfer analysis of lateral perforated fin heat sinks," *Appl. Energy*, vol. 86, no. 10, pp. 2019–2029, 2009.
[19] M. R. Shaeri and M. Yaghoubi, "Thermal enhancement from heat sinks by using perforated fins," *Energy Convers. Manag.*, vol. 50, no. 5, pp. 1264–1270, 2009.
[20] A. N. bin Samsudin, A. S. Tijani, S. T. Abdulrahman, J. Kubenthiran, and I. K. Muritala, "Thermal-hydraulic modeling of heat sink under force convection: Investigating the effect of wings on new designs," *Alexandria Eng. J.*, vol. 65, pp. 709–730, 2023.
[21] Abbas, A.S., Dawood, S.D. (2018). STudy Heat Diffusion Of Different Prosthetics. ARPN Journal of

Research Article

Engineering and Applied Sciences, 13(22), 8633-8641.4.
[22] Abbas, A.S., Mohammed, A.A. (2023). Enhancement of Plate-Fin Heat Exchanger Performance with Aid of (RWP) Vortex Generator. International Journal of Heat and Technology, 41(3), 780-788.
[23] H. Y. Li and K. Y. Chen, "Thermal-Fluid Characteristics of Pin-Fin Heat Sinks Cooled by Impinging Jet," *J. Enhanc. Heat Transf.*, vol. 12, no. 2, pp. 189–201, 2005, doi: 10.1615/JENHHEATTRANSF.V12.I2.40.
[24] S. A. E. Sayed Ahmed *et al.*, "Heat transfer performance evaluation in circular tubes via internal repeated ribs with entropy and exergy analysis," *Appl. Therm. Eng.*, vol. 144, no. June, pp. 1056–1070, Nov. 2018, doi: 10.1016/j.applthermaleng.2018.09.018.
[25] Jebir, S.K., Abbas, N.Y., Khudheyer, A.F. (2020). Effect of different nanofluids on solar radiation absorption. Journal of Mechanical Engineering Research and Developments, 44(1), 190-206.